

Self-powered Infusion Micropump Fabrication using Xurography and Thermal Lamination Techniques

Zul Fadhli Idris¹, Ummikalsom Abidin^{1*}, Nur Shamimi Amirah Md Sunhazim¹

¹School of Mechanical Engineering, Faculty of Engineering,
Universiti Teknologi Malaysia, 81310 UTM Johor Bahru, Johor, MALAYSIA

*Corresponding Author

DOI: <https://doi.org/10.30880/ijie.2022.14.02.006>

Received 30 April 2021; Accepted 30 September 2021; Available online 02 June 2022

Abstract: Point of care testing (POCT) as part of diseases and health monitoring will be very beneficial in resource constrained areas with minimum healthcare expert and power requirement. Elimination of external power source in testing device brought the idea of self-powered infusion micropump. This research aimed to fabricate and investigate the pumping capability of non-mechanical self-powered infusion micropump under the effect of different porous materials. The self-power infusion micropump was successfully fabricated with Xurography and thermal-lamination techniques. The average percentage difference between the measured dimensions of micropump with actual design was 2.30 %. Sandwich layers configuration of the micropump which consisted of PVC sheet and laminating plastic pouch was successfully fabricated and proven to have a leak-proof micropump. Micropump's flow rate of 0.89, 3.62, and 0.84 $\mu\text{L}/\text{min}$ were obtained under the effect of porous material ashless grade Whatman filter paper number W40, W41 and W42 respectively. These flow rate values were influenced by filtration speed as per porous material specifications.

Keywords: Point-of-care testing (POCT), micropump, xurography, thermal lamination

1. Introduction

Development of microfluidic technology have gained significant attention from researcher and scientist due to its benefits and wide range of application especially in biomedical field such as smaller sample sizes used and less time is required to perform the analysis. Furthermore, this technology provides very accurate results and allows precise parameter monitoring as the small size element studied enhances the potential for high-resolution separations and detections [1]. Nowadays, self-powered infusion micropump is used to eliminate the usage of external power supply, which is expensive and making the control of the device become more complex, to pump liquid in microchannel. There are several developments has been made on the self-powered infusion micropump which includes capillary forces, degas-driven and paper-based micropump.

Capillary pump used capillary actions to displace liquids and can be defined as the movement of liquids through a small channel due to adhesive and cohesive forces acting between the liquid and the surface [2]. It was initially introduced by Zimmermann et al. and from his study, the performance of capillary system was investigated by testing a range of capillary pumps [3]. In 2011, Liang et al. developed a degas-driven flow micropump, where the micropump takes advantage of the inherently high porosity and air solubility of PDMS by removing air molecules from the bulk PDMS before initiating the flow [4]. Another self-powered micropump is introduced by Martinez et al. using paper or porous materials as the pumping elements as it is low in cost, available everywhere, has wicking properties, compatible with biological sample, and disposable [5]. Even though these concepts of self-powered micropump had successfully been developed, they are still numerous limitations and drawbacks that need to be improved. The concept of capillary system as micropump has a limitation where the flow rate is influenced by ambient temperature and humidity [6] while the paper-based micropump is lacking several important abilities including ability to store, mix and combining reagents.

Due to the limitations mentioned earlier, Dosso et al. presented a new self-powered micropump where the liquid is being pushed through a microfluidic network, known as infusion micropump [7]. This new concept of self-powered micropump has two major benefits, in which it could drastically increase the complexity of liquid manipulations on autonomous lab-on-chip platforms and significantly expand the number of microfluidic applications.

In early year, the fabrication of lab-on-a-chip device is made up of silicon and glass by using micromachining techniques. Even though both materials have their own advantages but the required facilities and equipment are limited and cannot be accessible to everyone. Thus, polymer has been used as an alternative material to replace silicon and glass due to its incorporation of high-resolution, flexibility, optical transparency, and biocompatibility [8]. Polymer is more economic, easier to fabricate and has a wide range of materials that can be chosen according to the specific requirements needed to fabricate the mold compared to silicon and glass [9]. The main disadvantage of using polymer in fabricating the mold is time-consuming and laborious. In order to tackle the disadvantages of using polymer, digital craft cutting (Xurography) and thermal lamination technique have been discovered. Xurography is a low-cost rapid fabrication technique which uses plotter cutter to form pattern onto polymer materials [10]. Previous studies of this technique have proved that it provides a wide range of manufacturing flexibilities and able to achieve average dimensional error below than 8 %. Microfluidic fabrication process by Xurography can be completed by lamination, a technique of bonding polymer material by applying heat or pressure. Configuration of microfluidic device fabricated by Xurography and lamination consists of interface layer, flow layer, and base layer [11]. These fabrication processes offer several advantages including cheap materials, simple process, fast fabrication time, controllable layer depths (depends on material thickness), and submillimeter features [12].

Yuen and Goral has showed the overall procedure of using Xurography and it has been proven to be more user-friendly, portable and cheaper compared to replica molding and laser cutting [13]. This can be supported with research done by Islam et al. mentioning that Xurography can reduce the time taken of the fabrication process and inexpensive [14]. Kokalj et al. and Dosso et al. used this technique in fabricating the microfluidic device. It is done by cutting the microfluidic channel by using digital craft cutter [7], [15]. Both studies had been successfully conducted as the sample liquid injected in the channel, managed to flow along the channel throughout the process. In this research, design of the self-powered infusion micropump was duplicated from the research done by Dosso et al. and the prototypes were fabricated by using Xurography and thermal lamination technique. Fabrication quality of the micropump prototypes were evaluated by characterizing the prototypes using microscope and the flow rates of sample liquid in different microchannel sections were analyzed in order to study the influence of different porous materials on the flow rate.

2. Experimental

2.1 Materials

PVC Rigid Sheet (0.22 mm thickness) and Adoro laminating film (0.15 mm thickness) were used as layers of micropump. Silhouette Cameo 3-4T wireless cutting machine is used to cut the microchannel on the PVC rigid sheet, where the customized design of the micropump and microchannel are generated from any AutoCAD software and converted into DXF file format. Whatman filter paper grades 40, 41, and 42 were utilized as porous materials. Each filter paper has their own pore size, which are 8 μm for grade 40, 20-25 μm for grade 41 and 2.5 μm for grade 42. Due to these differences, the absorption rate and liquid flow are also varied. Two food colouring were used and each colour was mixed with tap water to provide a clearer visual of the liquids flowing along the channel during the experiment. Plasticine dough functioned as stopper to close the inlet hole in order to prevent any backflow of the liquids to happen. Other materials involved include HDPE gloves and micro fiber clothes, which were used as surface care of micropump layers and syringe to inject the liquids inside the channel.

2.2 Fabrication Method

Fabrication began by drawing the self-powered infusion micropump using computer-aided design (CAD) software (SolidWorks 2018, USA). Some changes has been made from the original design, where the size of the border has been increased by 1 cm for both height and width to minimize possible tear that may occur during the lamination process. Figure 1 shows the pattern of middle PVC layer of micropump where most significant dimensions were included in the figure. The thickness of the micropump is determined from the PVC rigid sheet used, which in my case was 220 μm . PVC rigid sheets were used as the middle layer of micropump, while laminating films were used as the top and bottom layer. By using digital cutter (Silhouette Cameo 3, USA), the pattern of self-powered infusion micropump layers were cut onto the PVC rigid sheet. Several try-and-error process have been done to determine the best input parameters in the digital cutter software for PVC rigid sheet. The cutting force, cutting speed and number of passes selected and set was 25, 3 cm/s and 2 respectively. Each parameter provides a different function, where the cutting force controls how hard the cutting blade is pressing down, cutting speed controls how fast the machine operates the cut and the number of passes signals the machine how many times it should cut the design. Once the desired design has been cut from the PVC rigid sheet, patterned PVC rigid sheet will be sandwiched and bonded between two laminating films by using thermal bonding or hot lamination machine at a temperature of 130 oC (Astar LM-230i, Malaysia), where the top layer was designed with inlet, outlet, and vent holes while the bottom layer act as the base of micropump. This

laminating film is coated with adhesive that will be activated when thermal heat is applied. Different grade of filter papers which were used as the porous material, were cut by digital cutter and then imbedded into the porous material chamber during the assembly of the micropump.

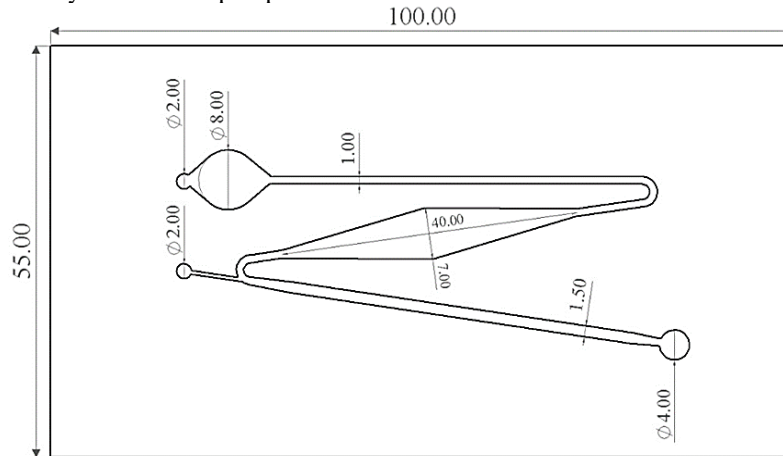


Fig. 1 - Design of micropump with exact dimensions (in mm)

2.3 Micropump Prefilling

Micropumps were prefilled with working liquid (blue dyed water) and sample liquid (red dyed water). The dyed water was prepared by mixing food colouring with water at 1:100 ratio. The working liquid is injected manually into the channel through the inlet hole by using syringe and stopped right before it reached the filter paper. Then, the sample liquid is injected the same way as working liquid but through the vent hole and stopped right before it reached the outlet hole. Once both liquids have been injected into the channel, the vent hole is closed by sticking the plasticine dough on top of it. Fig. 2 shows the prefilled micropump.

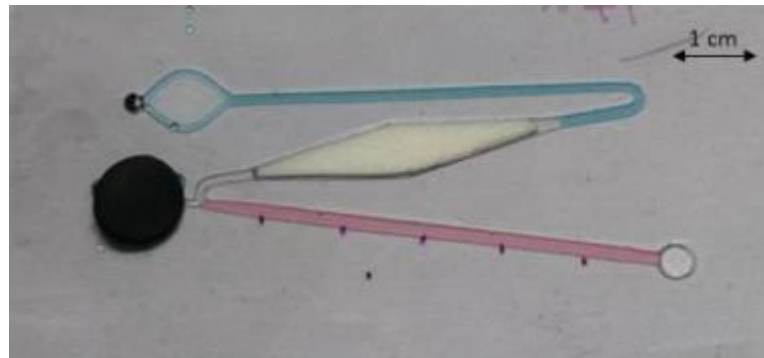


Fig. 2 - Prefilled micropump with working liquid (blue dyed water) and sample liquid (red dyed water)

2.4 Experimental Setup

Nine sample of micropumps with 3 different filter paper grades were fabricated, where each grade of filter paper will have 3 prototype samples. In order to study the fabrication quality of micropump, one of the samples was selected to be observed under the digital microscope and comments of the inspection were made on quality of cut and flowing liquid. Dimensions of different sections (width of working liquid channel, diameter of inlet hole, width of sample liquid channel, and diameter of outlet hole) of micropump middle layer were measured by using digital microscope (RaxVision, USA). Dimensional error was calculated using percentage difference formula. Phone camera (Apple iPhone 8, USA) was used to record the pumping of micropump prototype. Flow rates of 9 micropump prototypes were measured. Sample liquid channel was divided into 5 sections with equal length (10 mm) each. Flow rates were measured by lapping the time taken for the liquids to reach each section.

3. Results and Discussion

3.1 Characterization of Xurography Technique

As the materials used in this experiment were not listed in the digital cutter software database, a try-and-error process was done on the unused PVC rigid sheet to determine the optimum settings parameters for the material in the software by varying the cutting speed, cutting force and number of passes. The channel was cut onto the PVC rigid

sheet and viewed under the microscope to study the cutting quality for each setting parameters. The example of quality can be seen from Fig. 3. There are three crucial channels that were captured from the microscope, which are the working liquid channel, sample liquid channel and inlet hole. From the figure, it can be seen that there are some wastes were stuck on the sheet during the cutting process. It can be removed by wiping the sheet using micro fiber cloth. Overall, it has been proven that the digital cutter used in this experiment, managed to cut various designs and shapes such as curve, straight and circular line if correct settings parameters are keyed in the software for specific materials used. To assess the viability of Xurography technique by using digital cutter (Silhouette Cameo 3, USA), dimensions of 4 different sections of micropump were measured on 3 samples of middle layer (PVC) and the results were compared with actual design. Average dimensional error was calculated and illustrated in Fig. 4. The graph in Figure 4 showed overcutting or undercutting variability on the samples of cut with overall average error of 2.30 %. In this experiment, linear or rounded features did not show a constant behaviour of undercutting or overcutting. From graph Fig. 2, undercut sections were Working Liquid Channel and Outlet Hole with linear and rounded features respectively. The overcut sections which were Inlet Hole and Sample Liquid Channel also have both rounded and linear features. Undercutting and overcutting issue presented in this research may be an effect of common cutting problems such as dull blade and improper handling technique [16].

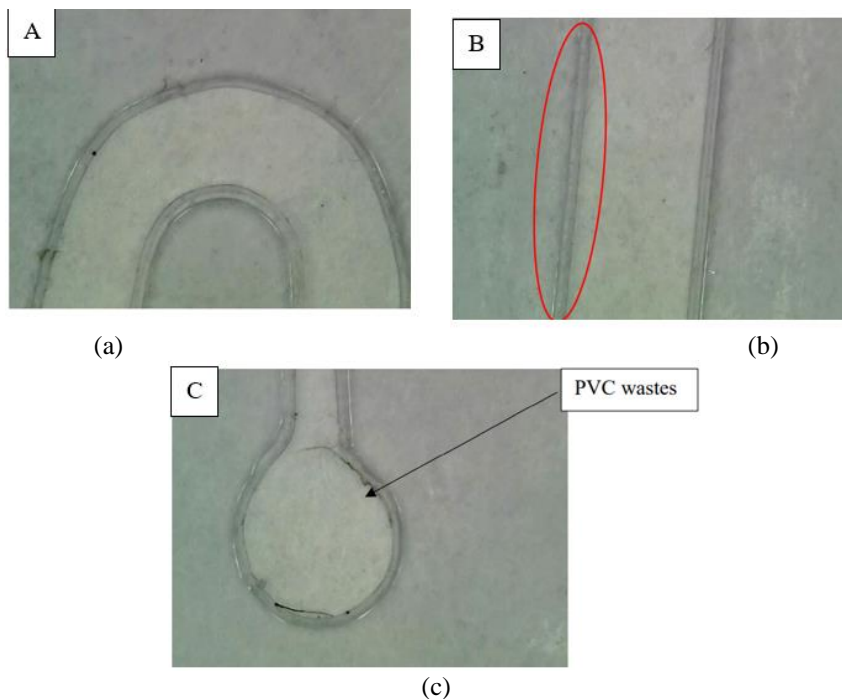


Fig. 3 - Captured image of the channel at: (a) curved working liquid channel; (b) sample liquid channel; (c) Inlet hole

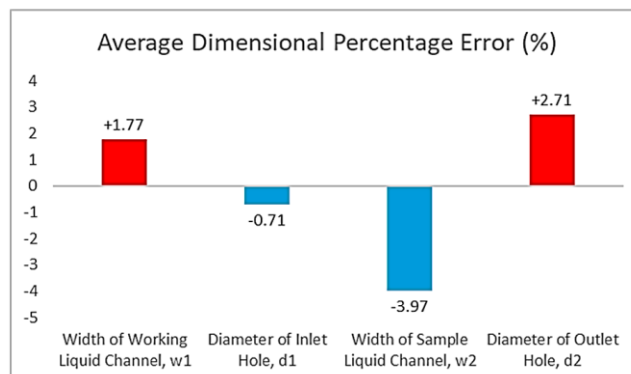


Fig. 4 - Average dimensional error of micropump; red represents overcutting while blue undercutting

During the thermal lamination process of the micropump, temperature should be set on the laminate machine. The manufacturer had specified ranges of laminating temperature based on the thickness of laminating film. For this project, laminating film with a thickness of 150 μm was used and the range of temperature suggested was between 130 $^{\circ}\text{C}$ to 150 $^{\circ}\text{C}$. The lamination process was tested with 130 $^{\circ}\text{C}$, 140 $^{\circ}\text{C}$, and 150 $^{\circ}\text{C}$ but the specimens did not show any

observable significant difference. Thus, constant temperature of 130 °C was used to laminate all the micropump prototypes. Some difficulties were identified during this process where the filter paper used, in a shape of diamond, cannot be easily fitted inside the desired chamber on the micropump prototype as it was designed to have only 0.05 mm tolerance. Other than that, the alignment for top and middle layer is very crucial as any mismatch between these two layers can cause vent or liquid cannot be injected into the inlet hole. Therefore, paper clip was used in minimizing misalignment of micropump by clipping the layers prior to rolling them into the laminating machine.

3.2 Pumping Capability of Micropump

Self-powered infusion micropump presented in this paper is similar to the previously developed micropump by Dosso et al., but the bonding technique used for this research was thermal lamination as opposed to pressure adhesive lamination used previously. Pumping capability of micropump was tested by activating the micropump after prefilling process. Figure 5 showed the snapshots of recorded pumping micropump from camera (Apple iPhone 8).

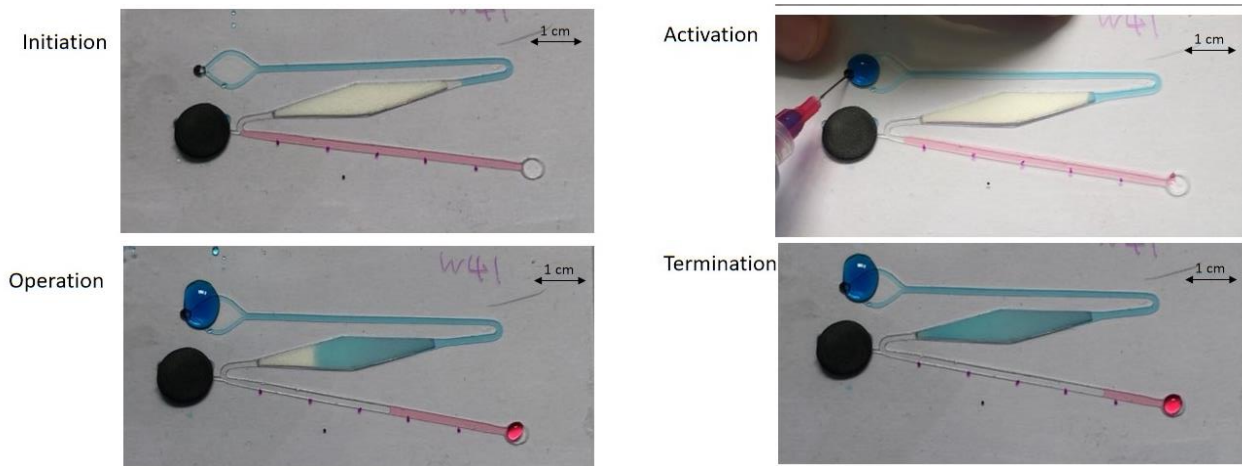


Fig. 5 - Pumping mechanism of micropump

Initially, pump is pre-filled with working liquid and sample liquid in the last step of fabrication and is ready to be used (Initiation). Subsequently, pump is activated with syringe injection, which causes the working liquid to touch the porous material and to increase the pressure on the sample liquid (Activation). Air expelled from the porous material pushes the sample liquid further in the sample liquid channel due to absorption (Operation). Finally, pumping terminates when either all the working liquid is absorbed in the porous material or when the porous material is saturated with working liquid. From Fig. 3, the micropump does not exhibit any leakage and the liquids were able to flow in the microchannels as intended. After the micropump has fully terminated, the microchannels of the micropumps are viewed under the microscope that is connected to the Inskam Android software. The view that managed to be captured from the microscope is presented as Fig. 6. According to Elveflow, possible causes of air bubbles trapped in microchannel are due to improper prefilling, leaking issue, and dissolved gas [17]. Since the micropump does not show any leaking and does not involve with gas flow, the reason for these air bubbles was improper prefilling. One needed to ensure that only liquid were contained in the syringe before injecting it into the channel. As for the case of unfit porous material, the tolerance of filter paper needed to be redesigned in order to make sure the paper fits properly inside the chamber. Proper handling technique is also required since the size of the fabrication is very small. Water liquids were stuck at the wall of channel due to low viscosity. Material selection of channel needed to be studied to ensure the liquid can flow effectively. Presence of impurities have also caused the liquid to stick at the wall due to absorption. This finding proved that it is important to clean the surface of micropump to minimize the effect of microstructure.

3.3 Effect of Different Filter Paper on Flow Rate

Three different filter papers (W40, W41, and W42) were used as the porous materials. Time taken for the sample liquids to reach each section (S1-2, S2-3, and S3-4) were recorded and the volumetric flow rate were calculated by assuming volume of each section is 3.3. The average flow rate of each section were graphed, as shown in Fig. 7. Based on graph in Fig. 7, the three filter papers tested (W40, W41, and W42) resulted in flow rates ranging from 0.7 to 4.5 $\mu\text{L}/\text{min}$ and all showed a decreased in the flow rate along with the pump operation. Filter paper W41 had the highest average flow rate at 3.62 $\mu\text{L}/\text{min}$, followed by W40 with 0.89 $\mu\text{L}/\text{min}$ and the lowest, W42 with 0.84 $\mu\text{L}/\text{min}$. Filtration speed W41 was described as “Fast Flow” with 54 s while W40 and W42 were described as “Medium Flow” with 340 s and “Slow Flow” with 1870 s respectively. It can be inferred that the lower the filtration speed Herzberg, the faster the absorption of liquid, which will result in higher flow rate. Therefore, the selection of filter paper can be based on the description of Fast, Medium, and Slow flow. These experiments proved that wide range of flow rates that can be

obtained with self-powered infusion micropump will depends on the selection of porous material. According to Dosso et al. [7], self-powered infusion micropump can provide faster or slower flow rate, depending on specific application, which gives a great advantage in liquid manipulation.

In addition, another property of filter paper used was the particle retention size. Retention size is the ideal diameter of the smallest particle blocked by the filter paper [18]. Each filter paper has their own particle retention size. Filter paper W40 has a particle retention size of 8 μm , while W41 and W42 are 20 – 25 μm and 2.5 μm respectively. According to the definition, smaller particle retention size means that the filter paper will have a smaller volume of voids and it will be more difficult to absorb liquids. From the experiment, W41 has the highest flow rate while W42 has the lowest flow rate. This is because W41 has the biggest particle retention size among the filter papers used. Thus, from the results obtained, it is concluded that bigger particle retention size will results in higher flow rates of sample liquid in microchannel.

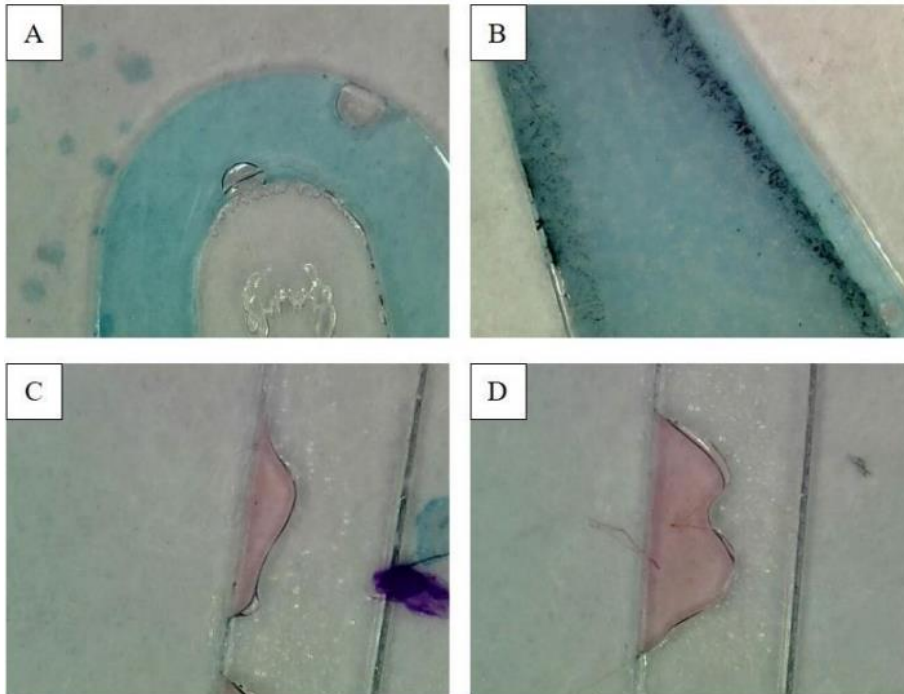


Fig. 6 - Microscopic viewed of micropump after Termination (a) Air bubbles trapped inside the microchannel; (b) Filter paper was not fit properly into the porous material chamber; (c) Some liquids stuck at the wall of channel; (d) Liquids were absorbed by impurities

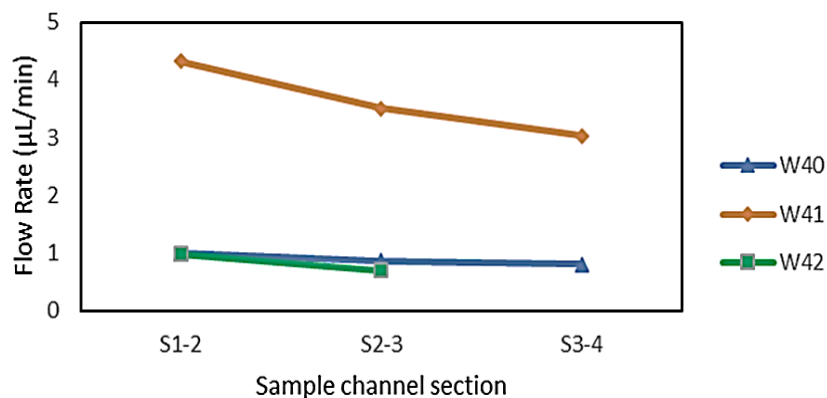


Fig. 7 - Schematic diagram for preparation of $\text{TiO}_2@\text{Ag}$ and Ag/TiO_2 microspheres

3.4 Percentage Difference

The same filter paper is used in previous study done by Dosso et al., [7] which was filter paper grade 40. Therefore, a percentage difference on the flow rate is calculated in order to verify the results obtained from the experiment. From Dosso et al., [7] it can be estimated that filter paper W40 used by their experiment were able to produce an average flow rate of 1.2 $\mu\text{L}/\text{min}$, while the average flow rate of filter W40 obtained from this experiment

was 0.89 $\mu\text{L}/\text{min}$. Percentage difference between these two experiments was calculated and the value obtained was 25.8 %. Possible reasons for this difference may be caused by the different in liquids used, modified mechanism of micropump pumping, and different bonding technique.

In previous experiment, distilled water was used as coloured water solution as opposed to tap water which were used in this experiment. Distilled water is preferred to be used in scientific experiments because they are inert, which means little to nothing remains in the water after distilling [19]. According to Brenner [19], tap water on the other hand contains chemicals, minerals, and metals that can affect the outcome of any research. Besides that, in Dosso et al., [7] the working liquid is stored in the reservoir at the inlet hole while for this experiment, the liquid is injected inside the channel by using syringe until the porous materials started to absorb the liquid. The technique used in both experiments was also different, where Dosso et al. [7] bonded the prototype device using adhesive and used PSA as their material for middle layer. Both of the Middle Layer surface have adhesive properties which can be adhered when pressure is applied. While in this experiment, the micropump prototype was bonded by thermal lamination using a roller laminate machine. Both techniques provided different pressure to bond the layers of the micropump, thus can cause slight deformation on the overall design and disturb the flow of liquids.

4. Conclusion

The self-powered infusion micropump requires no external power activation. Fabrication method by Xurography and thermal lamination has been proven to have no leakage on the microchannels. The process of fabrication is simple and easy; no complex or specialized equipment is required. The accuracy of digital cutting was evaluated, and the average dimensional error was only 2.30 %. Manipulation of flow rates were tested by using different grade of filter paper (W40, W41, and W40) and the flow rates obtained ranging from 0.7 to 4.5 $\mu\text{L}/\text{min}$. The selection of filter paper, depending on specific flow rates application, can be based on the description of filtration speed. For future works, characterization of Xurography technique shall be further studied by investigate the effect of different cutting parameters (speed, force, number of passes) on the measured dimension. Moreover, other filter paper grades shall be assessed to increase the variation of flow rates.

Acknowledgement

I would like to thank Ministry of Education Malaysia for the Fundamental Research Grant Scheme, FRGS/1/2019/TK03/UTM/02/2 and Universiti Teknologi Malaysia in supporting this research.

References

- [1] Thomas, L. (2019). Benefits of using a microfluidic device. *News: Medical Life 51 Sciences*, 1–4. Retrieved from <https://www.news-medical.net/life-sciences/Benefits-of-a-Microfluidic-System.aspx>
- [2] Helmenstine, A. M. (2020). Capillary Action: Definition and Examples. *Study.Com*, 1–2. Retrieved from <https://study.com/academy/lesson/capillary-action-of-water-definition-examples-lesson.html>
- [3] Zimmermann, M., Schmid, H., Hunziker, P., & Delamarche, E. (2007). Capillary pumps for autonomous capillary systems. *Lab on a Chip*, 7(1), 119–125.
- [4] Liang, D. Y., Tentori, A. M., Dimov, I. K., & Lee, L. P. (2011). Systematic characterization of degas-driven flow for poly(dimethylsiloxane) microfluidic devices. *Biomicrofluidics*, 5(2), 1–16.
- [5] Martinez, A. W., Phillips, S. T., Whitesides, G. M., & Carrilho, E. (2010). Diagnostics for the developing world: Microfluidic paper-based analytical devices. *Analytical Chemistry*, 82(1), 3–10.
- [6] Guan, Y. X., Xu, Z. R., Dai, J., & Fang, Z. L. (2006). The use of a micropump based on capillary and evaporation effects in a microfluidic flow injection chemiluminescence system. *Talanta*, 68(4), 1384–1389.
- [7] Dal Dosso, F., Kokalj, T., Belotserkovsky, J., Spasic, D., & Lammertyn, J. (2018). Self-powered infusion microfluidic pump for ex vivo drug delivery. *Biomedical Microdevices*, 20(2), 1–11.
- [8] Faustino, V., Catarino, S. O., Lima, R., & Minas, G. (2016). Biomedical microfluidic devices by using low-cost fabrication techniques: A review. *Journal of Biomechanics*, 49(11), 2280–2292.
- [9] Wu, J., & Gu, M. (2011). Microfluidic sensing: State of the art fabrication and detection techniques. *Journal of Biomedical Optics*, 16(8), 1–13.
- [10] Martinez-Lopez, J. I., Mojica, M., Rodriguez, C. A., & Siller, H. R. (2016). Xurography as a rapid fabrication alternative for point-of-care devices: Assessment of passive micromixers. *Sensors (Switzerland)*, 16(5), 1–21.
- [11] Ontiveros, F., & McDowell, J. R. (2016). Ultra-thin microfluidic devices built via thermal lamination. *International Conference on Nanochannels, Microchannels and Minichannels*. Washington, United States of America. 1–63.
- [12] Gale, B. K., Jafek, A. R., Lambert, C. J., Goenner, B. L., Moghimifam, H., Nze, U. C., & Kamarapu, S. K. (2018). A review of current methods in microfluidic device fabrication and future commercialization prospects. *Inventions*, 3(3), 60, 1–25.

- [13] Yuen, P. K., & Goral, V. N. (2010). Low-cost rapid prototyping of flexible microfluidic devices using a desktop digital craft cutter. *Lab Chip*, 10(3), 384–387.
- [14] Islam, M., Natu, R., & Martinez-Duarte, R. (2015). A study on the limits and advantages of using a desktop cutter plotter to fabricate microfluidic networks. *Microfluidics and Nanofluidics*, 19(4), 973–985
- [15] Kokalj, T., Park, Y., Vencelj, M., Jenko, M., & Lee, L. P. (2014). Self-powered imbibing microfluidic pump by liquid encapsulation: SIMPLE. *Lab Chip*, 14(22), 4329–4333.
- [16] Clark, J. (2012). Troubleshooting common cutting problems. PostPress Website. Retrieved from <https://postpressmag.com/articles/2012/troubleshooting-common-cutting-problems/>
- [17] Elve, F. (2020). Air bubbles and microfluidics: Tips and tricks to remove them. Elvesys Website. Retrieved from <https://www.elveflow.com/microfluidicreviews/general-microfluidics/air-bubbles-and-microfluidics/>
- [18] Fluted, F. (2020). Retention vs Pore Size. Fluted Filter Website. Retrieved from <http://www.flutedfilter.com/blog/retention-vs-pore-size/>
- [19] Brenner, L. (2018). Why Is Distilled Water a Good Control for Science Projects? Sciencing website. Retrieved from <https://sciencing.com/distilled-good-control-science-projects-7418493.html>